Development of a ReaxFF Force Field for Aqueous Phosphoenolpyruvate as a Novel Biomimetic

Carbon Capture Absorbent

Yihan Huang^a, Anthony S. Wexler^{b,c,d,e}, Keith J. Bein^{c,f}, Roland Faller^{g*}

^a Department of Materials Science and Engineering, ^bAir Quality Research Center, ^c Department of Mechanical and Aerospace Engineering, ^d Department of Civil and Environmental Engineering, ^e Department of Land, Air and Water Resources, ^f Center for Health and the Environment, and ^g Department of Chemical Engineering, University of California, Davis, CA, USA 95616

* Correspondence: rfaller@ucdavis.edu

KEYWORDS:

Carbon capture, ReaxFF parametrization

Abstract

Phosphoenolpyruvate (PEP) found in C₄ plants could be a novel green absorbent in biomimetic carbon capture through its Crassulacean Acid Metabolism (CAM) mechanism, and could

potentially substitute the most commonly used absorbent Monoethanolamine in future post-combustion capture systems. In this study, a new ReaxFF model has been developed to describe the CAM reactions involving PEP and the atomic interactions in the P/C/O/H system. The ReaxFF force field parameters were fitted against quantum mechanical (QM) training data for partial charges, molecular structures, bond dissociation energies, reaction energies and activation energies. 2nd generation water parameters were combined with P/C parameters for more accurate water description and P's electrostatic parameters were specially treated to correct P/O interactions. The developed P/C/O/H ReaxFF model was able to reproduce the training set for structures and energetics of the molecules and reactions involved in the CAM process, and accurately describe the aqueous bicarbonate and PEP systems. Molecular dynamics simulation using this ReaxFF model depicts how bicarbonate reacts with PEP and in solution and determines the impact of local structure on reactions necessary to perform carbon capture using PEP, which enables the potential design of PEP variant as the optimal carbon capture absorbent.

1. Introduction

Greenhouse gas emissions are the primary cause of climate change, which is the existential challenge of this century. Most human activities consume energy and in the current energy economy most of that energy is generated by combustion of fossil fuels, which releases significant amounts of CO₂, the major greenhouse gas, into the air. Carbon capture and storage (CCS) technologies encompass a suite of approaches that either remove CO₂ from the flue gas or from the atmosphere itself to reduce emissions or reduce atmospheric concentrations, respectively. ¹⁻³ This process encompasses capturing CO₂ from gas mixtures and then liquefying it so that it can be transferred and stored underground. ⁴⁻⁵ For large-scale applications, the most prevalent form of CSS is post-combustion capture (PCC) wherein CO₂ is removed from the flue gas in an absorber.

Currently, this is the preferred form of CCS as it does not require additional steps prior to combustion; therefore, is straightforward to integrate into existing infrastructure.⁶⁻⁷ Monoethanolamine (MEA) is an amine compound which is a commercially available and most frequently used CO₂ solvent in PCC. It typically captures 85% to 90% of the CO₂ produced. ⁴ The benchmark solvent for regenerative chemical absorption-based PCC in terms of cost, energy penalty, CO₂ capture efficiency, and physicochemical properties is a 30wt% aqueous solution of MEA. ⁸⁻⁹ While typically benign, MEA as a PCC absorbent suffers from thermal and chemical degradation and high energy production cost. ¹⁰⁻¹¹ MEA can break down at high temperatures or when released into the atmosphere forming toxic vapors. ¹² In addition, MEA contains nitrogen that is derived by nitrogen fixation from the atmosphere such that producing MEA is energy intensive. These shortcomings have prompted a search for alternative CO₂ solvents that are nontoxic and less energy intensive to produce and use for PCC.

Phosphoenolpyruvate (PEP) is found in C₄ plants that use Crassulacean Acid Metabolism for their photosynthesis and are adapted to arid climates. ¹³ At night when its cooler and more humid, the plants open their stoma to uptake CO₂ that immediately reacts with PEP, to store CO₂ overnight. ¹⁴ In the morning when the sun rises and temperatures increase, the stoma close, and the reaction is reversed releasing CO₂ to participate in photosynthesis. ¹⁵ To utilize this chemistry in PCC, CO₂ would dissolve in an aqueous solution of PEP, the carbon dioxide would dissolve in this solution forming bicarbonate, which in turn would attack the phosphate group in PEP and split PEP into a carboxyphosphate and the enolate form of pyruvate (Figure 1). ¹⁶ Based on this concept, PEP could serve as a novel green absorbent in biomimetic CCS and could potentially serve as template for designing similar molecules to substitute MEA in future PCC systems. In order to

further examine the viability of PEP as a CCS solvent requires detailed knowledge of its thermodynamics and kinetics when reacting with bicarbonate.

Computation can be an effective and efficient tool to study the chemistry of this system, and to screen possible PEP variants. In addition, understanding the thermodynamics and kinetics of PEP may assist investigations into the biochemistry and metabolism of C4 plants. Quantum mechanics (QM) -based methods like density functional theory (DFT) ¹⁷⁻¹⁸ are powerful tools to describe chemical reactions on the atomistic scale. However, these calculations are very computationally expensive and thus limit the available time scale and length scales. On the other hand, empirical force field methods like classical molecular dynamics (MD) simulations can study the system's dynamic evolution over nano- to microseconds with tens to hundreds of thousands of atoms but loses the reaction information since the atom connectivity has to be normally predefined. In order to describe the reaction in Figure 1 and evaluate potential PEP variants, we use ReaxFF-based reactive MD that fills in the gap between quantum chemistry and classical empirical force fields.

Little prior work has examined reaction of phosphate-containing molecules. The closest example is that by Zhang and coworkers 22 who developed a ReaxFF model for carbon capture that uses ionic liquids (ILs) to capture CO_2 mixtures. The chosen IL was tetrabutylphosphonium glycinate, $[P(C_4)_4]$. Although it contains the atoms P, C, O, and H, it was not parametrized for the system and chemistries of our interest, and the phosphorus was bonded to four carbons instead of oxygens like in the PEP system here. Furthermore, phosphorus in $[P(C_4)_4]$ does not participate in the reaction, so this force field does not necessarily describe P-O bond formation and breakage accurately. In addition, the H/O interaction parameters were from the 1^{st} generation water force field from which NPT water density is known to be significantly smaller than the experimental value, and the H_2O ,

H₃O⁺, and OH⁻ diffusion constants are in incorrect order. ²³ We deal with an aqueous system so the water behavior needs to be more accurate than the 1st generation water force field. A force field that could accurately describe both the physical and chemical interactions between bicarbonate and PEP in water is needed. In this work, we develop a ReaxFF force field for PEP-based carbon capture, compare against partial charges, molecule structures, and energetics of molecules in vacuum, and then validate and predict molecular behavior in solutions.

2. Computational Methods

2.1 ReaxFF formalism

ReaxFF is a reactive force field that allows bond formation and dissociation. The total system energy is comprised of bond order dependent energies as well as non-bonded energies. ¹⁹⁻²⁰ Unlike in classical empirical force fields, each chemical element is represented by only one atom type, and its connectivity is not predefined but derived from bond orders (BO) that are functions of interatomic distances at every MD step. As formulated in the bond order equation in Figure 2, the bond order between a pair of atoms consists of three exponential terms, each corresponding to the sigma bond ($p_{bo,1}$ and $p_{bo,2}$) which is unity below ~ 1.5 Å but negligible above ~ 2.5 Å, a first pi bond ($p_{bo,3}$ and $p_{bo,4}$) which is unity below ~ 1.2 Å but negligible above ~ 1.75 Å, and a second pi bond ($p_{bo,5}$ and $p_{bo,6}$) which is unity below ~ 1.0 Å but negligible above ~ 1.4 Å. ¹⁹ So, for example, as two carbon atoms starting from very close contact separate, the bond order gradually drops from three (triple bond) to zero (fully dissociated). Like in a classical force field, the van der Waals and Coulomb interactions are also included for all atom pairs, where a shielding term is used to avoid excessively close range non-bonded interactions, and polarization effects are calculated through a geometry dependent charge equilibrium scheme. ²⁴⁻²⁵

The ReaxFF force field ff.P/N/C/O/H/Na originally developed by Zhang and coworkers ²² was used as the starting parameter set in our optimization. All water related parameters were replaced with those from the 2nd generation water force field ²³ and kept fixed during parametrization. C and P atomic parameters and C-C, C-O and O-P interaction parameters were re-parametrized to better describe the reaction in Figure 1. Table 1 shows which parameters are chosen based on their physicochemical importance to our system.

The optimization process works in two stages: training set generation and a parallel search algorithm. (26) New parameter values are accepted such that they reduce the error between training set features and ReaxFF fitted features. Figure 3 shows the workflow. A detailed description of the algorithm can be found in Deetz' work. 26 The scripts we are using are written in MATLAB and Bash, and the parallel search optimization part is run in parallel on a high performance cluster (HPC1/2 at UC Davis). The goal is to minimize the error function P (Figure 3), in which the inverse weights ω_i for each feature in the training set are selected so that each section of the training set (e.g., charges, reactions) weighs similarly into the overall error function. Then after the error function converges, weights were readjusted according to the sectional errors or even the individual feature errors to fine-tune the parameters and focus on the ones which most deviate from the target while making sure to not negatively impact the others. This process was repeated until the overall performance of the new force field matches the training set with acceptable errors, and the most important features like the kinetics matches the training data very well.

2.2 Training set generation

The training set has four sections – charge, geometry, energy, and reaction. DFT calculations were performed to acquire the necessary information using Gaussian 16 ²⁷, and the relaxed structures were fed to LAMMPS (release version 12 Dec 2018) ²⁸⁻²⁹ that runs the MD simulations

to calculate the error function. The charge and geometry sections collect the partial charges, bond lengths, and angles of the neutral forms of bicarbonate, PEP, carboxyphosphate, enolate, oxaloacetate, the transition state, as well as their charged states. The transition state refers to the reaction where the PO₃²⁻ group dissociates from the charged PEP³⁻ (Figure 4a). Since the molecules were all in vacuum for DFT calculations, and the intermediate species in Figure 1 is not stable in vacuum, it was excluded from the training set. Because LAMMPS requires a neutral system, counter ions were introduced into the system to balance the anions. The reactions happen in aqueous water, which will self-ionize into H₃O⁺ and OH⁻, so to keep the nature of environment and prevent any unrelated reactions, H₃O⁺ were inserted as counter ions. H₃O⁺ were placed at least 4 Å away from the anions to avoid unwanted interactions. Figure 4b shows an example of such a neutralized system with PEP³-, other systems are shown in Figure S1. The Becke, 3-parameter, Lee-Yang-Parr functional (B3LYP) 30-31 and the basis set 6311++g(d,p) 32-33 were used in DFT calculations to simulate the geometrically optimized structures,. In order to be consistent with charge equilibrium for ReaxFF, 19 a Mulliken charge calculation population analysis 34 with B3LYP/631g(d,p) 35 was used to calculate partial charges. The bond section collects the bond dissociation energy scans for P-O and O-H bonds in neutral PEP and carboxyphosphate. The reaction section has the reaction energy of the bicarbonate (HCO₃⁻) + PEP (H₂C₃O₆P³⁻) \rightarrow carboxyphosphate (HCO₆P²⁻) + enolate form of pyruvate (H₂C₃O₃²⁻) reaction and the activation energy of the splitting of PEP³⁻ into PO₃²⁻ and the enolate form of pyruvate. The DFT activation energy and the energies along the reaction pathway of the splitting of PEP³⁻ were obtained from intrinsic reaction coordinate (IRC) ³⁶⁻³⁷ scans. H₃O⁺ were again added to neutralize, and B3LYP/6311++g(d,p) was used to calculate energies.

2.3 Charge parameter correction

An intrinsic problem with the force field before re-parametrization was that the atomic hardness parameter (etaEEM in the force field notation) of phosphorous made it too "soft", so that when the intermediate species formed, P donated too many electrons to the double bonded O, leading to extreme partial charges +8.6e and -7.2e, respectively, after a few steps in the MD runs. The theoretical partial charges of the P=O pair were +1.2e and -0.7e respectively. This created a huge unphysical local dipole that eventually led to simulation instability and stopped the reaction. This only occurred during the dynamic runs when the reacting PEPs are in solution, so the parametrization process that trained the parameters against static DFT values in vacuum could not address this problem, and a special treatment on the etaEEM parameter of P was needed. The etaEEM parameter of P after standard parametrization was 7.2562, and so a snapshot was taken just before the huge dipole formed and etaEEM of P was set to be 5, 6, 7, 8, and 9 and partial charges were calculated. It was found that when etaEEM of P was 8, the partial charges of the P=O pair were +0.85e and -0.65e respectively, which were closest to the theoretical values, and the intermediate species did not break. Finally, the force field was fine-tuned with etaEEM of P starting at 8 and was only allowed to take very small scaling steps during the fine-tuning. The final etaEEM of P was 7.9960 and the partial charges of the P=O pair were +1.05e and -0.70e, respectively, and these values kept the simulation stable.

2.4 MD simulation

All MD simulations were performed in LAMMPS. Because the benchmark solvent for chemical absorption-based PCC is 30wt% MEA, 24 PEPs were randomly distributed in 520 waters to create a 30wt% PEP solution. PEPs were kept in their neutral form during equilibration. Counter ions were used to ensure charge neutrality. Similarly, bicarbonates initially were in their neutral form (carbonic acid). Pressure fluctuations converted some carbonic acids to CO₂, so in order to have

enough bicarbonates to react with PEP, 36 bicarbonates were randomly distributed. Therefore, the initial box contained 520 H₂O, 24 neutral PEP, 36 carbonic acid, 108 H₃O⁺ and 108 OH⁻, and was first equilibrated in the canonical (NVT) ensemble for 20 ps at 300 K, and then equilibrated in the isothermal-isobaric (NPT) ensemble for another 25 ps at 300 K and 1 atm. A short equilibration time ensured less reactions during equilibration. Temperature was maintained using a Nosé-Hoover thermostat ³⁸ with a damping parameter of 25 fs, and pressure was maintained using a Nosé-Hoover barostat with a damping parameter of 250 fs. Then 18 H⁺ were deleted from 6 PEP to create 6 PEP³⁻, 9 H⁺ were deleted from 9 carbonic acid to create 9 bicarbonate, together with 27 OH⁻, and the system was equilibrated in NPT for 10 ps to eliminate potential unphysical dipoles created by the deletions. This deletion and equilibration process was repeated 4 times. Then the resulting system was simulated as reaction stage for 2 ns in NPT at 300 K and 1 atm. Time steps of 0.25 fs were used for all the NVT and NPT runs.

3. Results and Discussion

3.1 Force field parametrization

The atomic partial charge errors between ReaxFF simulations and QM calculations are negligible, and the bond and angle errors are all less than 6% and 8%, respectively (Figure 5). Bond dissociation energy scans in Figure 6 (a-c) show good agreement. O-P, C-O, and O-H bonds at the active sites for both neutral PEP and neutral carboxyphosphate were scanned from very short to equilibrium distances and then to very large distances without relaxing the whole structure, and the energies along the scans were acquired. To account for the multiple spin states as the molecules break, both singlet and triplet scans were calculated, and the lower energies were taken. Some energy data points at far distances were removed to reduce computational cost. The structures corresponding to each DFT data point along the scans were then fed to ReaxFF MD simulations

to calculate ReaxFF energies. Figure S2 shows additional bond dissociation energy scans. The fitted ReaxFF energies generally match the DFT energies, especially at the regions near the equilibrium distances, and the performance of the force field improved substantially comparing to the original one.

Figure 6 (d) shows the comparison of the energies along the reaction pathway and the reaction energy between DFT (B3LYP/6311++g(d,p)) and ReaxFF. The energies along the reaction pathway were obtained from intrinsic reaction coordinate (IRC) calculation using DFT, and the ReaxFF energies were fitted using for the structures along the DFT IRC curve. The barrier energy from DFT and ReaxFF are 8.87 kcal/mol and 7.08 kcal/mol, respectively, and the reaction energy from DFT and ReaxFF are -16.90 kcal/mol and -12.84 kcal/mol, respectively. Both the barrier energy and the reaction energy prove that the optimized force field can well describe the kinetics and thermodynamics of the reaction.

3.2 Solution validation

Diffusion coefficients and radial distribution functions (RDFs) were also calculated (Figure 7) and compared with literature values³⁹ using non-reactive MD simulations to characterize HCO_3^- , and PEP^{3-} in water. Diffusion coefficients were obtained by fitting to the mean square displacement (MSD) over the time interval where MSD increased linearly. The diffusion coefficient of HCO_3^- at 298 K in Zeebe's work was $1.17 \times 10^{-9} m^2 s^{-1}$, and the diffusion coefficient of HCO_3^- at 298 K in our ReaxFF fitted system was $0.67 \times 10^{-9} m^2 s^{-1}$. Because both calculations were performed on one HCO_3^- in water, a statistical error was expected, and the discrepancy between the two diffusion coefficients were acceptable particularly as our model was not optimized for dynamics.

The RDF of HCO₃⁻ was calculated both in Zeebe's work and in our system. The first peak of the RDF between the carbon in HCO₃⁻ and the oxygen in H₂O was around 3.65 Å in the ReaxFF system whereas between carbon in HCO₃⁻ and hydrogen in H₂O around 2.57 Å in the ReaxFF fitted system. Both matched with Zeebe quantitatively. In addition, the RDFs of H₂CO₃, PEP³⁻ and PEP were also calculated. Diffusion coefficients and RDFs compared between the non-reactive MD simulations in Zeebe's work and our ReaxFF model show that the model not only correctly describes vacuum properties but also solution structure and dynamics.

3.3 Analysis and prediction

After optimization and initial validation (see above) long simulations were performed for 30wt% PEP in water with bicarbonate using the newly parametrized ReaxFF model ff.P/C/O/H (see Supplementary Information). Depending on the initial configuration, the reaction sometimes proceeds very easily and sometimes was not observed after the 2 ns runs showing that local structure is important for reaction progress. In the runs where the reactions happened, the species in Figure 1 were observed. For example, in one case (Figure 8), two intermediate species were formed, weakening the two P-O bonds where the oxygens connect to the carbons. Then one of the intermediate species dissociates into an enolate form of pyruvate and a carboxyphosphate, which then diffuse away from each other, making both the enolate form of pyruvate and the carboxyphosphate stable. These reactions match with the expected reactions (Figure 1), showing that the developed ReaxFF model predict the correct reactions without need for biasing.

The correlation between the partial charges and the reaction was also analyzed. For the system where two PEP-bicarbonate pairs reacted, the partial charge and the coordination number of P in the reacting PEPs were recorded over 25 ps (Figure 9 a-b). The coordination number of P in stable PEP was 4, but when the PEP reacted with a bicarbonate to form the intermediate, the P connected

with an oxygen from the bicarbonate raising its coordination number to 5. It was observed that the partial charge of the P in the reacting PEP was negatively correlated with the coordination number. The P in the reacting PEP has lower partial charge when it bonded to the O in the bicarbonate.

In another run where only one PEP-bicarbonate pairs reacted, the partial charge and coordinate number of that P were recorded, and those of the P in 10 randomly chosen non-reacting PEPs were also recorded for comparison (Figure 9 c-d). We observe that the P in non-reacting PEPs generally had higher partial charges than in the reacting PEP, and in the non-reacting PEPs, the partial charge of the P did not have any correlation with the coordination number of the Ps. Therefore, if the PEP reacts with its neighboring bicarbonate, the partial charge of its P tends to be lowered and is negatively correlated with its coordination number.

4. Conclusion

We developed a ReaxFF model ff.P/C/O/H for biomimetic carbon capture potentially using PEP as a substitute for MEA. During the force field parametrization, we found out that the phosphorous' EEM parameters have some intrinsic problems that needed to be treated. The final ReaxFF model was able to correctly predict vacuum properties of the molecules and reaction related to our target carbon capture chemistries, as well as solution properties. The developed model also correctly predicted the target reactions during MD simulations, where bicarbonates react with PEPs in solution to form the intermediate species and then dissociate into the carboxyphosphate and enolate form of pyruvate. We also observed that if the PEP reacts with its neighboring bicarbonate, the partial charge of its P tends to be lowered and is negatively correlated with its coordination number. Thus, we have developed a model which can determine the impact of local structure on reactions necessary to perform carbon capture using PEP. This will enable selection of optimal reaction

conditions and design of new PEP variants that are more reactive with bicarbonate, more stable after reaction, and possibly more energy-efficient.

Figure 1. Chemistry of bicarbonate reacting with PEP in water.

$$E_{\text{system}} = E_{\text{bond}} + E_{\text{over}} + E_{\text{under}} + E_{\text{val}} + E_{\text{tors}} + E_{\text{Hbond}} + E_{\text{vdWaals}} + E_{\text{Coulomb}}$$

$$E_{\text{bond}} = \text{bonded interaction}$$

$$E_{\text{over}} = \text{penalty for over coord.}$$

$$E_{\text{under}} = \text{stabilize under coord.}$$

$$E_{\text{under}} = \text{stabilize under coord.}$$

$$E_{\text{val}} = \text{valence angle interaction}$$

$$E_{\text{Coulomb}} = \text{Coulomb interaction}$$

$$E_{\text{Coulomb}} = \text{Coulomb interaction}$$

$$E_{\text{coulomb}} = \text{Coulomb interaction}$$

$$E_{\text{val}} = \text{valence angle interaction}$$

$$E_{\text{coulomb}} = \text{Coulomb interaction}$$

$$E_{\text{coulomb}} = \text{Coulomb interaction}$$

$$E_{\text{coulomb}} = \text{Coulomb interaction}$$

Figure 2. The fundamental equations of ReaxFF formulism.

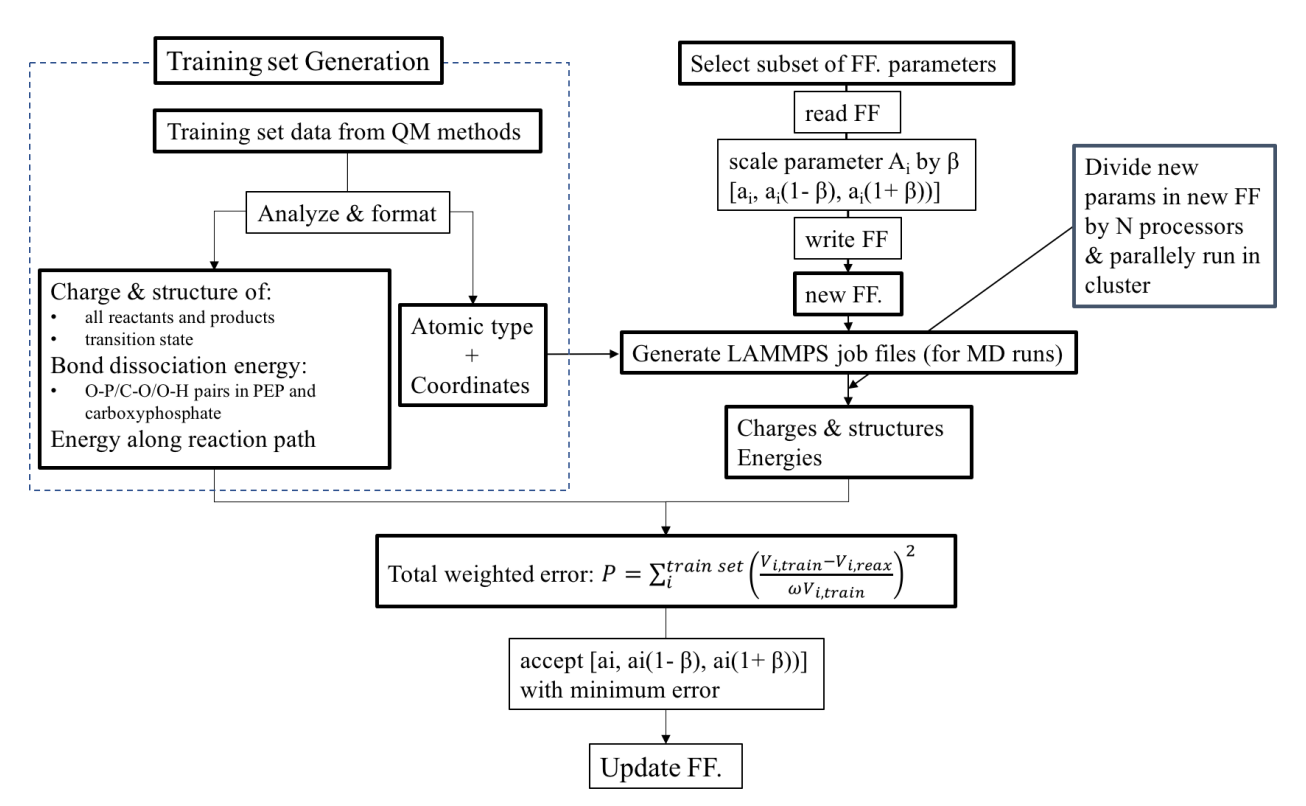


Figure 3. Workflow of the whole optimization process.

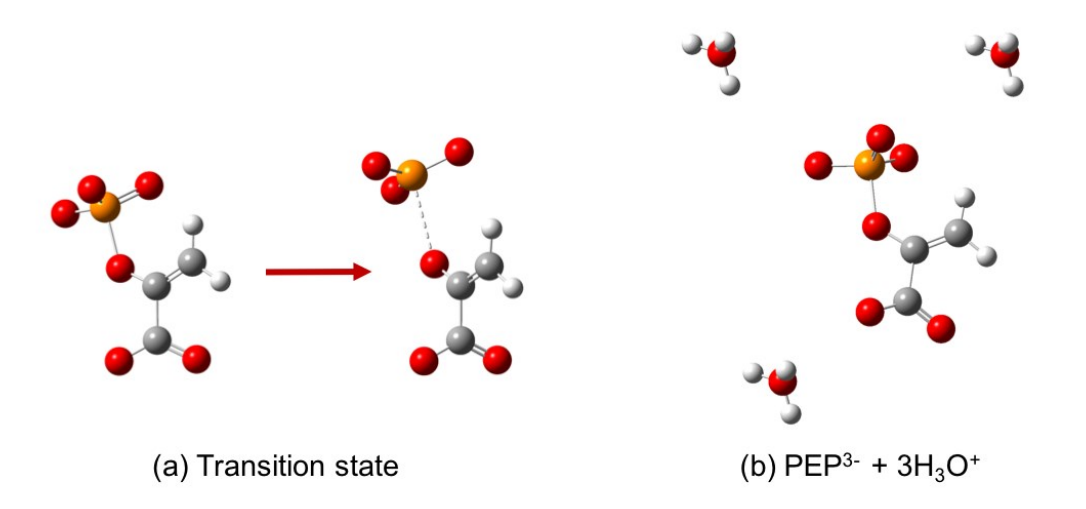


Figure 4. (a) transition state of the dissociation of PEP³⁻, and (b) the neutralized system of charged PEP³⁻.

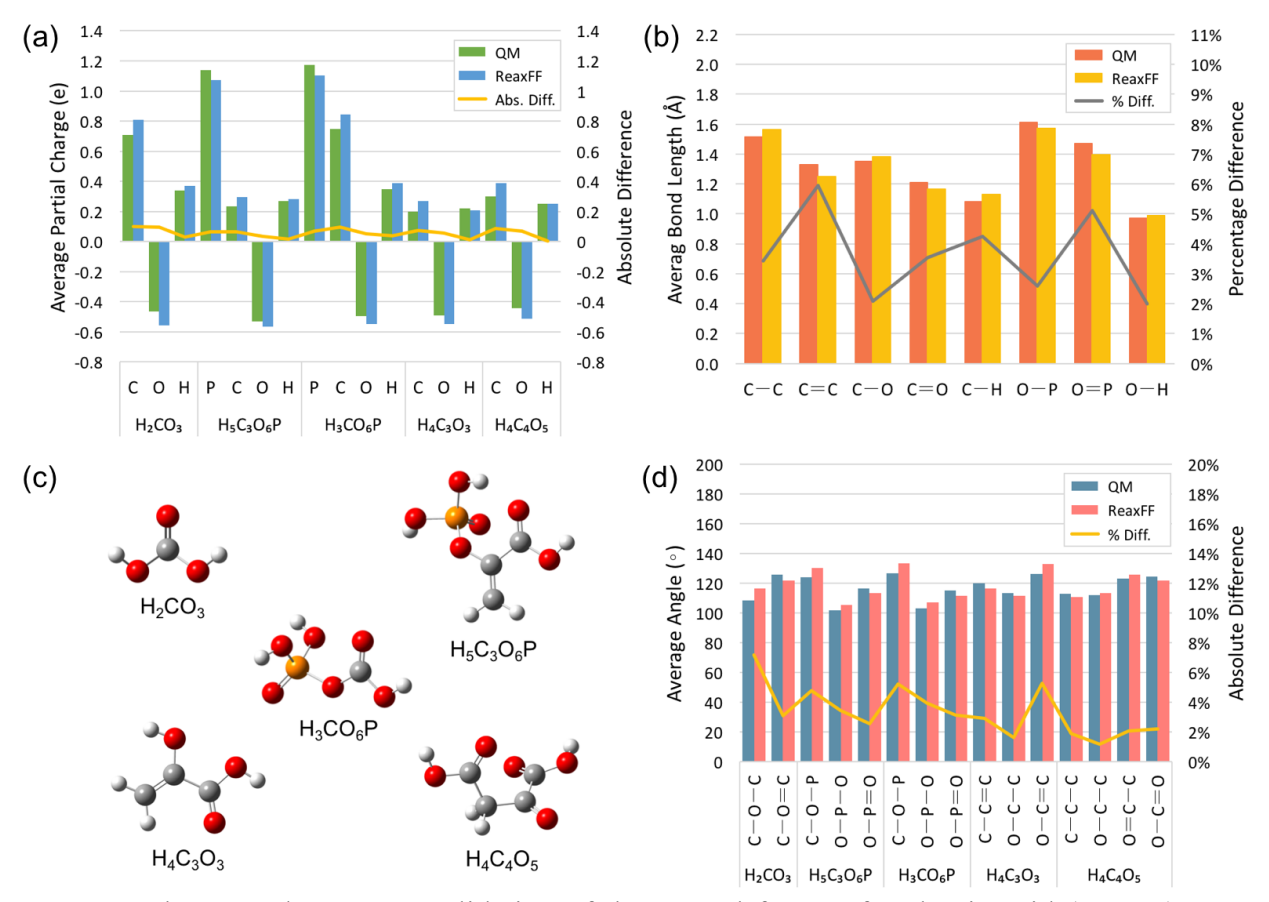


Figure 5. Charge and structure validation of the neutral forms of carbonic acid (H₂CO₃), PEP (H₅C₃O₆P), carboxyphosphate (H₃CO₆P), enolate form of pyruvate (H₄C₃O₃), and oxaloacetate (H₄C₄O₅). (a): average partial charge comparison between ReaxFF and QM for all atoms; (b): average bond length comparison between ReaxFF and QM for all type of bonds; (d): average angle comparison between ReaxFF and QM for bonds around active sites in each molecule; (c): representations of the neutral forms of the molecules. Tables with direct number comparisons are in Supplementary Information.

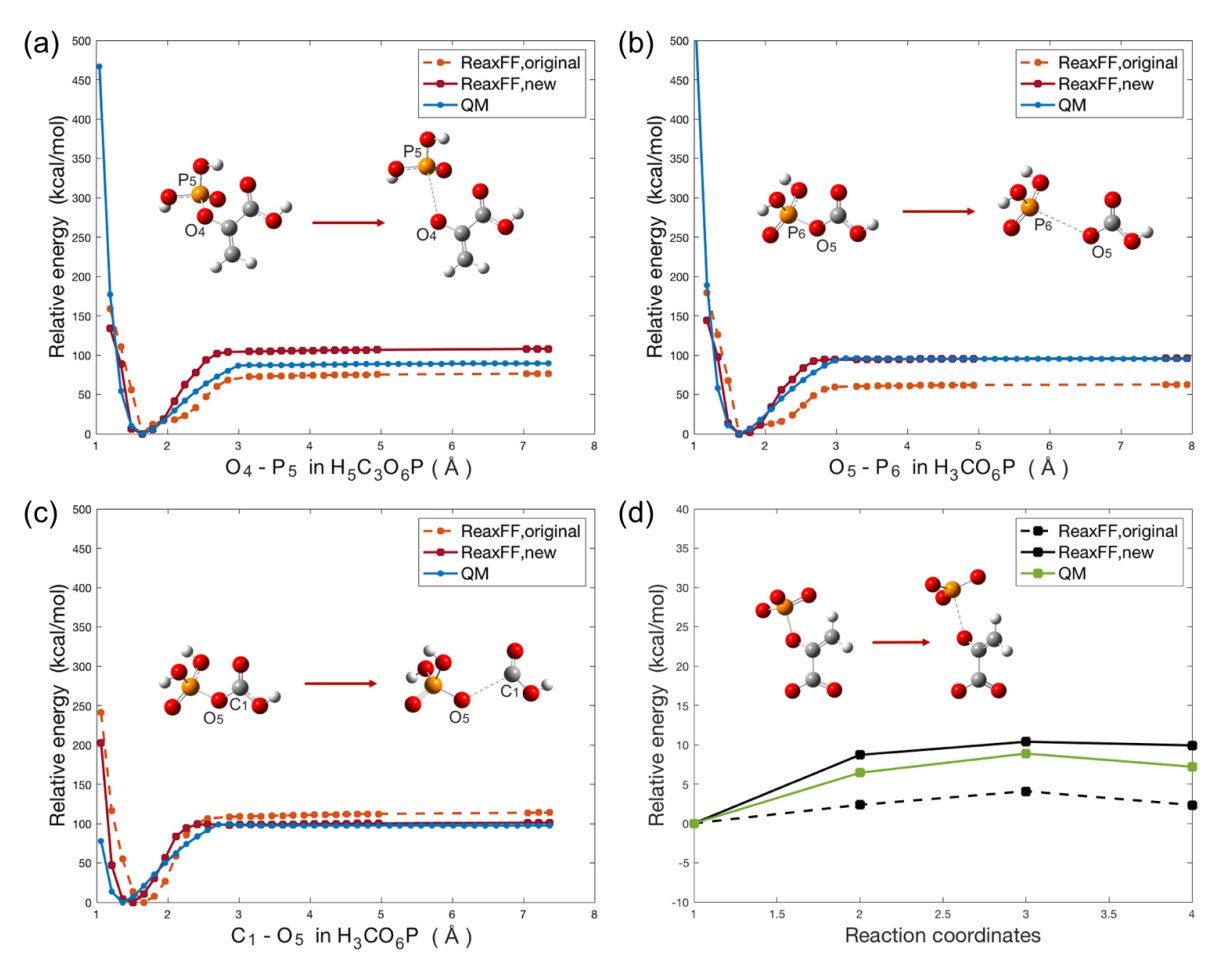


Figure 6. (a-c): bond dissociation energy scans comparison between DFT and ReaxFF. Blue represents bond dissociation energy scans from DFT calculations, orange represents the ReaxFF force field before re-parametrization, and red represents ReaxFF after the re-parametrization; (d): intrinsic reaction coordinate (IRC) from DFTvs ReaxFF with barrier and reaction energies. Green represents the IRC from DFT, and black represents ReaxFF fitted values, among which the dash line represents the force field before re-parametrization, and the solid line represents the new ReaxFF after re-parametrization.

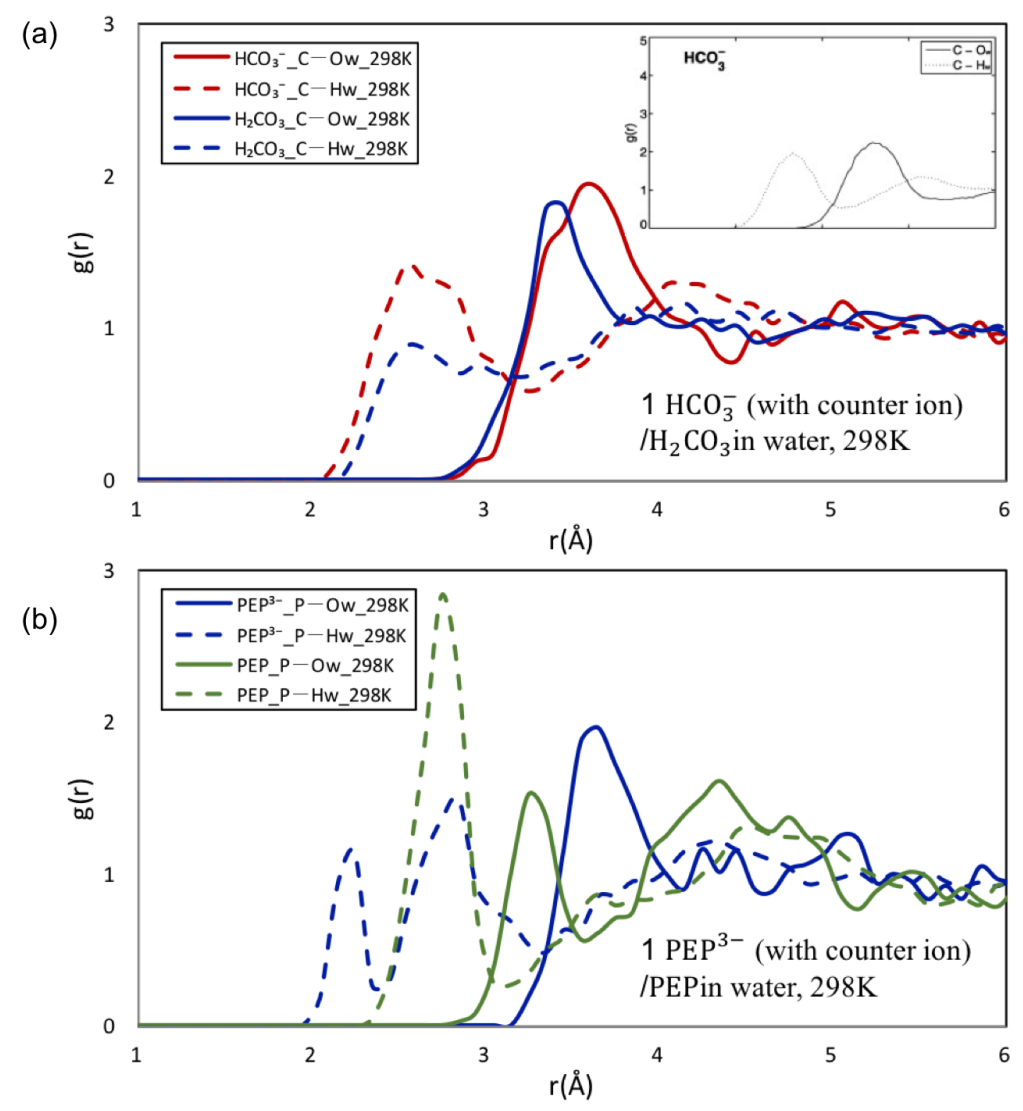


Figure 7. RDFs of 1 target molecule in water at 298 K. (a): RDF of HCO₃⁻ and H₂CO₃; (b): RDF of PEP³⁻ and PEP. The inset was reprinted from Geochimica et Cosmochimica Acta, volume 75, issue 9, Richard E. Zeebe et al., On the molecular diffusion coefficients of dissolved CO₂, HCO₃⁻, and CO₃²⁻ and their dependence on isotopic mass, Pages No. 16, Copyright (2011), with permission from Elsevier.

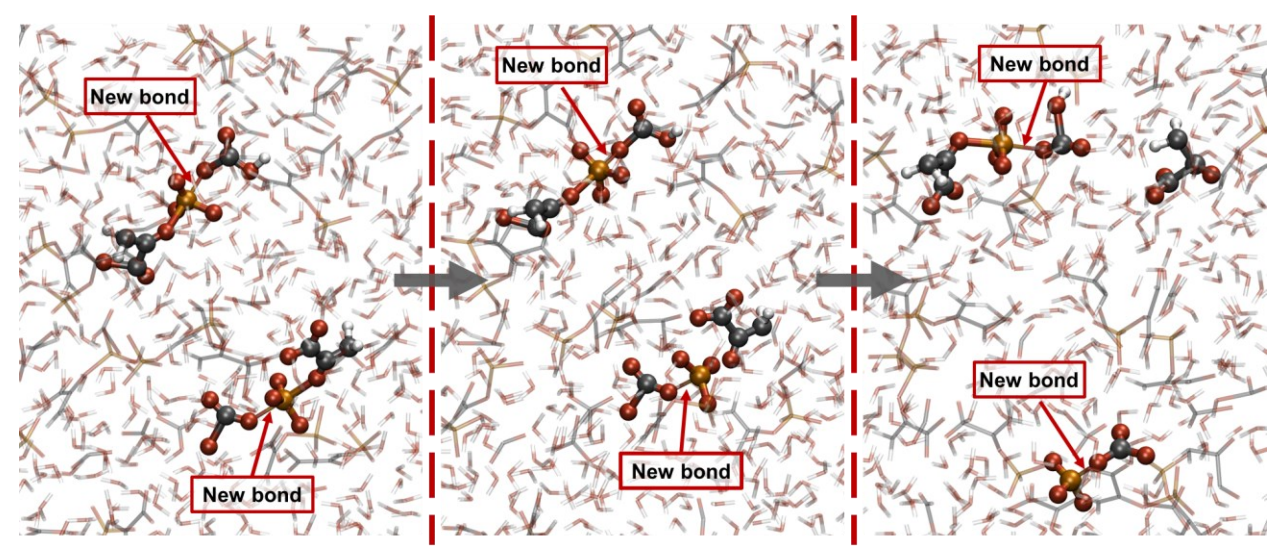


Figure 8. snapshots of three different stages of the reactions in one of the runs. The thinner P-O bond indicates the newly formed P-O bond.

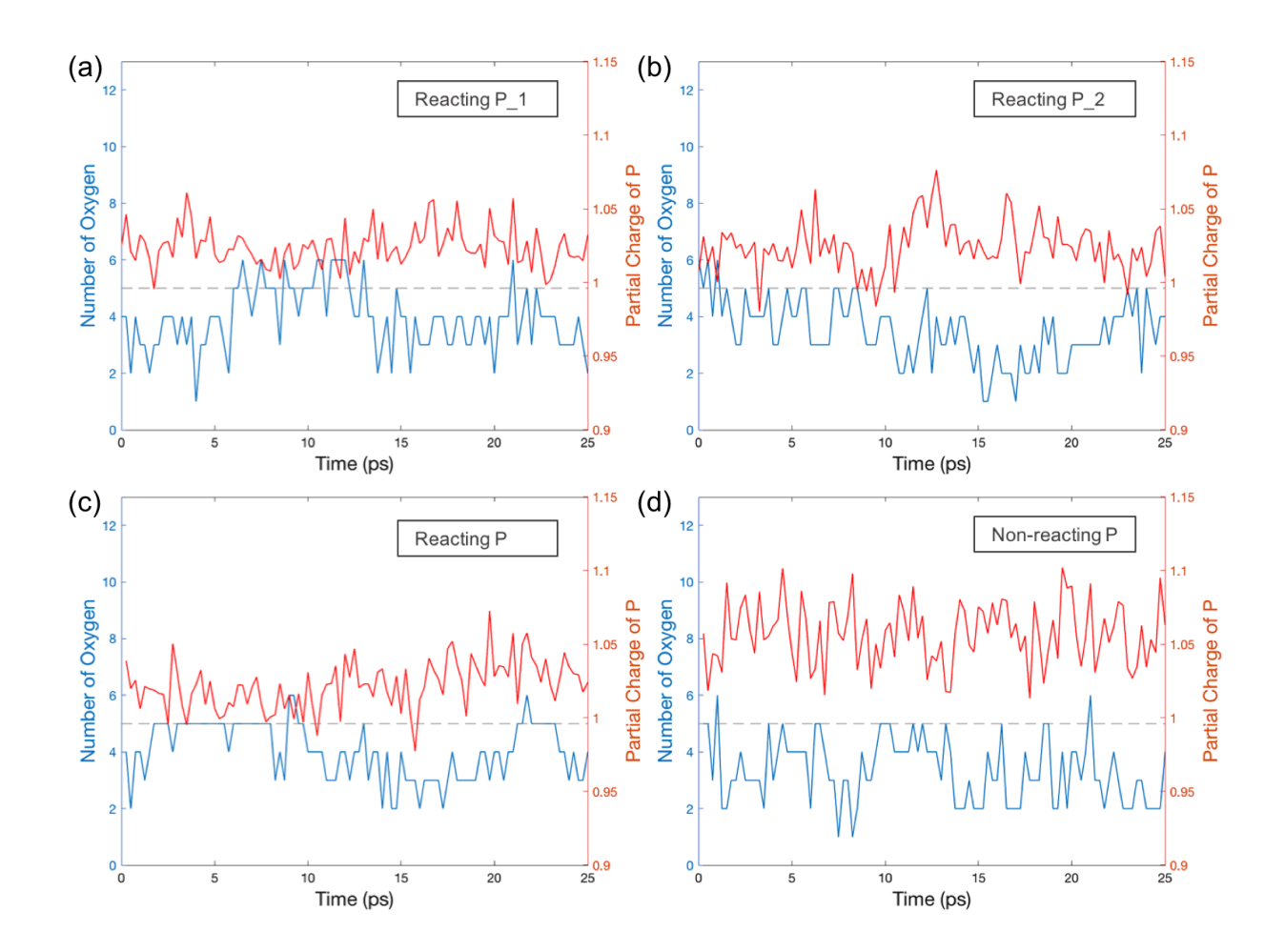


Figure 9. partial charges (red) and coordination number of P (blue) in reacting PEPs where there were two reacting PEP-bicarbonate pairs (a-b) and in both reacting and non-reacting PEPs where there were only one reacting PEP-bicarbonate pairs (c-d). The dash line corresponds to coordination number equals 5.

	Parameters chosen	Reasons for chosen
Electrostatic	Electronegativity equalization method (EEM) parameters for C, P	Bonding prediction
Valence bond	All bond radii/order/dissociation energy, under/over coordination energy parameters for C, P atoms and C-C, C-O, P-O pairs	Bonding prediction
		Reaction pathway
		Reactant/product/transition state structure
Valence angle	All angle parameters of C, O, P related angles in the molecules	Geometry prediction
Van der Waals	Vdw radii/dissociation energy/shielding for C,P	Bonding prediction

Table 1. Choice of optimized force field parameters.

ASSOCIATED CONTENT

Supporting Information.

The following files are available free of charge.

Supporting Data and Figures.pdf (file type, i.e., PDF):

Fig S1: The neutralized systems of all the charged molecules used in the training set

Table S1: Averaged partial charges calculated from the parametrized ReaxFF model against quantum mechanical (QM) method (ie. DFT).

Table S2: Averaged bond lengths calculated from the parametrized ReaxFF model against quantum mechanical (QM) method (ie. DFT).

Table S3: Averaged angles calculated from the parametrized ReaxFF model against

quantum mechanical (QM) method (ie. DFT).

ffield.reax.P_C_O_H.pdf (file type, i.e., PDF)

Final force field

AUTHOR INFORMATION

Corresponding Author

* Correspondence: rfaller@ucdavis.edu

Author Contributions

The manuscript was written through contributions of all authors. All authors have given approval

to the final version of the manuscript.

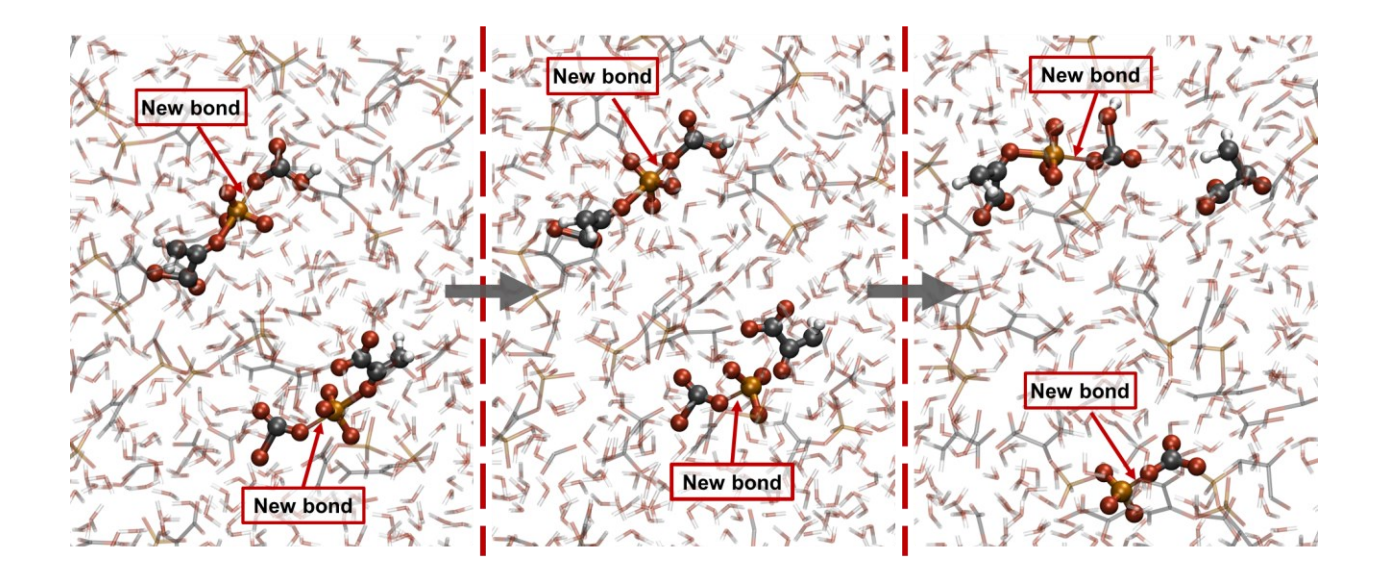
ACKNOWLEDGMENT

We thank Francois Gygi for many fruitful discussions. Parts of this work was supported by the

National Science Foundation grant CBET 1911267. Additional funding from the California

Energy Commission (EPC-2015-072) and the Electric Power Research Institute (EPRI) is

acknowledged.



TOC graphic

REFERENCES

- (1) Bui, M.; Adjiman, C. S.; Bardow, A.; Anthony, E. J.; Boston, A.; Brown, S.; Fennell, P. S.; Fuss, S.; Galindo, A.; Hackett, L. A., Carbon Capture and Storage (CCS): The Way Forward. *Energy Environ. Sci.* **2018**, *11*, 1062-1176.
- (2) Raza, A.; Gholami, R.; Rezaee, R.; Rasouli, V.; Rabiei, M., Significant Aspects of Carbon Capture and Storage—a Review. *Petroleum* **2019**, *5*, 335-340.
- (3) Tcvetkov, P.; Cherepovitsyn, A.; Fedoseev, S., Public Perception of Carbon Capture and Storage: A State-of-the-Art Overview. *Heliyon* **2019**, *5*, e02845.
- (4) Wilberforce, T.; Baroutaji, A.; Soudan, B.; Al-Alami, A. H.; Olabi, A. G., Outlook of Carbon Capture Technology and Challenges. *Sci. Total Environ.* **2019**, *657*, 56-72.
- (5) Kelemen, P.; Benson, S. M.; Pilorgé, H.; Psarras, P.; Wilcox, J., An Overview of the Status and Challenges of CO₂ Storage in Minerals and Geological Formations. *Frontiers in Climate* **2019**, *1*, 9.
- (6) Koperna Jr, G. J.; Gupta, N.; Godec, M.; Tucker, O.; Riestenberg, D.; Cumming, L., Society of Petroleum Engineers Grand Challenge: Carbon Capture and Sequestration. **2016**. https://www.spe.org/en/industry/carbon-capture-sequestration-2016/? ga=2.127508813.1521841451.1651901470-1675539005.1651901470
- (7) Council, N. P., Meeting the Dual Challenge—a Roadmap to at-Scale Deployment of Carbon Capture, Use, and Storage. National Petroleum Council Washington, DC: 2019.
- (8) Lepaumier, H.; da Silva, E. F.; Einbu, A.; Grimstvedt, A.; Knudsen, J. N.; Zahlsen, K.; Svendsen, H. F., Comparison of MEA Degradation in Pilot-Scale with Lab-Scale Experiments. *Energy Procedia* **2011**, *4*, 1652-1659.
- (9) Feron, P. H.; Cousins, A.; Jiang, K.; Zhai, R.; Garcia, M., An Update of the Benchmark Post-Combustion CO₂-Capture Technology. *Fuel* **2020**, *273*, 117776.
- (10) Supap, T.; Idem, R.; Tontiwachwuthikul, P.; Saiwan, C., Kinetics of Sulfur Dioxide-and Oxygen-Induced Degradation of Aqueous Monoethanolamine Solution During CO₂ Absorption from Power Plant Flue Gas Streams. *Int. J. Greenh. Gas Control* **2009**, *3*, 133-142.
- (11) Chi, S.; Rochelle, G. T., Oxidative Degradation of Monoethanolamine. *Industrial & engineering chemistry research* **2002**, *41*, 4178-4186.
- (12) Lee, D.; Wexler, A. S., Atmospheric Amines Part III: Photochemistry and Toxicity. *Atmos. Environ.* **2013**, *71*, 95-103.
- (13) Sage, R. F.; Sage, T. L.; Kocacinar, F., Photorespiration and the Evolution of C4 Photosynthesis. *Annu. Rev. Plant Biol.* **2012**, *63*, 19-47.
- (14) Sutton, B., The Path of Carbon in CAM Plants at Night. Funct. Plant Biol. 1975, 2, 377-387.
- (15) Nimmo, H. G., The Regulation of Phosphoenolpyruvate Carboxylase in CAM Plants. *Trends Plant Sci.* **2000**, *5*, 75-80.
- (16) Vidal, J.; Chollet, R., Regulatory Phosphorylation of C4 Pep Carboxylase. *Trends Plant Sci.* **1997**, *2*, 230-237.
- (17) Parr, R. G.; Yang, W., Density-Functional Theory of the Electronic Structure of Molecules. *Annu. Rev. Phys. Chem.* **1995**, *46*, 701-728.
- (18) Parr, R. G.; Yang, W., Density Functional Approach to the Frontier-Electron Theory of Chemical Reactivity. *J. Am. Chem. Soc.* **1984**, *106*, 4049-4050.
- (19) Van Duin, A. C.; Dasgupta, S.; Lorant, F.; Goddard, W. A., ReaxFF: A Reactive Force Field for Hydrocarbons. *J. Phys. Chem. A* **2001**, *105*, 9396-9409.

- (20) Chenoweth, K.; Van Duin, A. C.; Goddard, W. A., ReaxFF Reactive Force Field for Molecular Dynamics Simulations of Hydrocarbon Oxidation. *J. Phys. Chem. A* **2008**, *112*, 1040-1053.
- (21) Senftle, T. P.; Hong, S.; Islam, M. M.; Kylasa, S. B.; Zheng, Y.; Shin, Y. K.; Junkermeier, C.; Engel-Herbert, R.; Janik, M. J.; Aktulga, H. M., The ReaxFF Reactive Force-Field: Development, Applications and Future Directions. *Npj Comput. Mater.* **2016**, *2*, 1-14.
- (22) Zhang, B.; van Duin, A. C.; Johnson, J. K., Development of a ReaxFF Reactive Force Field for Tetrabutylphosphonium Glycinate/CO₂ Mixtures. *J. Phys. Chem. B* **2014**, *118*, 12008-12016.
- (23) Zhang, W.; Van Duin, A. C., Second-Generation ReaxFF Water Force Field: Improvements in the Description of Water Density and OH-Anion Diffusion. *J. Phys. Chem. B* **2017**, *121*, 6021-6032.
- (24) Mortier, W. J.; Ghosh, S. K.; Shankar, S., Electronegativity-Equalization Method for the Calculation of Atomic Charges in Molecules. *J. Am. Chem. Soc.* **1986**, *108*, 4315-4320.
- (25) Rappe, A. K.; Goddard III, W. A., Charge Equilibration for Molecular Dynamics Simulations. *J. Phys. Chem.* **1991**, *95*, 3358-3363.
- (26) Deetz, J. D.; Faller, R., Parallel Optimization of a Reactive Force Field for Polycondensation of Alkoxysilanes. *J. Phys. Chem. B* **2014**, *118*, 10966-10978.
- (27) Frisch, M.; Trucks, G.; Schlegel, H.; Scuseria, G.; Robb, M.; Cheeseman, J.; Scalmani, G.; Barone, V.; Petersson, G.; Nakatsuji, H., Gaussian 16. Gaussian, Inc. Wallingford, CT: 2016.
- (28) Thompson, A. P.; Aktulga, H. M.; Berger, R.; Bolintineanu, D. S.; Brown, W. M.; Crozier, P. S.; in't Veld, P. J.; Kohlmeyer, A.; Moore, S. G.; Nguyen, T. D., Lammps-A Flexible Simulation Tool for Particle-Based Materials Modeling at the Atomic, Meso, and Continuum Scales. *Comput. Phys. Commun.* **2022**, *271*, 108171.
- (29) Aktulga, H. M.; Fogarty, J. C.; Pandit, S. A.; Grama, A. Y., Parallel Reactive Molecular Dynamics: Numerical Methods and Algorithmic Techniques. *Parallel Comput.* **2012**, *38*, 245-259.
- (30) Becke, A. D., Density-Functional Exchange-Energy Approximation with Correct Asymptotic Behavior. *Phys. Rev. A* **1988**, *38*, 3098.
- (31) Lee, C.; Yang, W.; Parr, R. G., Development of the Colle-Salvetti Correlation-Energy Formula into a Functional of the Electron Density. *Phys. Rev. B* **1988**, *37*, 785.
- (32) McLean, A.; Chandler, G., Contracted Gaussian Basis Sets for Molecular Calculations. I. Second Row Atoms, Z= 11–18. *J. Chem. Phys.* **1980**, *72*, 5639-5648.
- (33) Krishnan, R.; Binkley, J.; Seeger, R; Pople, J.A., Self-consistent molecular orbital methods. XX. A basis set for correlated wave functions *J. Chem. Phys* **1980**, *72*, 650-654.
- (34) Mulliken, R. S., Electronic Population Analysis on LCAO–MO Molecular Wave Functions. I. *J. Chem. Phys.* **1955**, *23*, 1833-1840.
- (35) Petersson, G.; Al-Laham, M. A., A Complete Basis Set Model Chemistry. II. Open-Shell Systems and the Total Energies of the First-Row Atoms. *J. Chem. Phys.* **1991**, *94*, 6081-6090.
- (36) Deng, L.; Ziegler, T.; Fan, L., A Combined Density Functional and Intrinsic Reaction Coordinate Study on the Ground State Energy Surface of H₂CO. *J. Chem. Phys.* **1993**, *99*, 3823-3835.
- (37) Deng, L.; Ziegler, T., The Determination of Intrinsic Reaction Coordinates by Density Functional Theory. *Int. J. Quantum Chem.* **1994**, *52*, 731-765.
- (38) Nosé, S., A Unified Formulation of the Constant Temperature Molecular Dynamics Methods. *J. Chem. Phys.* **1984**, *81*, 511-519.

(39) Zeebe, R. E., On the Molecular Diffusion Coefficients of Dissolved CO₂, HCO₃-, and CO₃²⁻ and Their Dependence on Isotopic Mass. *Geochim. Cosmochim. Acta* **2011**, *75*, 2483-2498.